

Photocatalytic Degradation of Chlorinated Ethanes in the Gas Phase on the Porous TiO₂ Pellets: Effect of Surface Acidity

Suzuko Yamazaki,* Keiko Ichikawa, Atsue Saeki, Toshifumi Tanimura, and Kenta Adachi

Division of Environmental Science and Engineering, Graduate School of Science and Engineering, Yamaguchi University, Yamaguchi 753-8512, Japan

Received: December 15, 2009; Revised Manuscript Received: March 12, 2010

The photocatalytic degradation of chlorinated ethanes was studied in a tubular photoreactor packed with TiO₂ pellets prepared by sol–gel method. The steady-state condition was not obtained, but the deterioration in the photocatalytic activity was observed during the irradiation. Effects of mole fractions of water vapor, O₂, and C₂H₅Cl or C₂H₄Cl₂ and reaction temperature on the photodegradation of C₂H₅Cl or C₂H₄Cl₂ were examined, and these data were compared with those obtained by the photodegradation of chlorinated ethylenes. On the basis of the products detected with and without oxygen in the reactant's gas stream, we proposed the degradation mechanism. Measurement of diffuse reflectance infrared Fourier transform spectroscopy of pyridine adsorbed on the catalysts showed that decrease in the conversion for the photodegradation of C₂H₅Cl was attributable to the formation of Brønsted acid sites. Comparison of the data obtained with the TiO₂ and the sulfated TiO₂ (SO₄²⁻/TiO₂) pellets indicated that the photodegradation of C₂H₅Cl was suppressed by the presence of the Brønsted sites, but that of trichloroethylene was not affected. Such a difference is attributable to the adsorption process of these reactants on the acid sites on the catalyst surface.

Introduction

Volatile chlorinated organic compounds (VCOCs) such as trichloroethylene (TCE) and trichloroethane have presented serious environmental concerns for several decades because they are toxic and carcinogenic to animals. Several methods are available to remove VCOCs from waste gas, such as adsorption on activated carbon, wet scrubbing, and catalytic oxidation. The former two methods only transfer VCOCs from gaseous phase to solid or liquid phase, whereas catalysis can destroy them.

Photodegradation of various pollutants by photocatalysis, using wide band gap semiconductors, has been widely studied. Among them, the TiO₂ photocatalysts have been of great interest because TiO₂ is stable, harmless, and inexpensive and potentially can be activated by solar energy.¹ In particular, studies on the gas-phase photocatalytic degradation of TCE have become an active field because many soils and groundwater supplies have been contaminated with TCE as a result of leaking underground storage tanks and improper disposable practices. The photocatalytic degradation of TCE to CO₂ and HCl on the TiO₂ has been studied by many researchers, and dichloroacetyl chloride, phosgene, and chloroform have been identified as byproducts.^{2–13} Most of these studies were conducted in a closed vessel. However, for developing as a practical remediation method for a contaminated gas, a flow system in a noncirculating mode, that is, single pass mode, is more appropriate. We performed kinetic studies on the photocatalytic degradation of chlorinated ethylenes such as ethylene chloride, TCE, and tetrachloroethylene (PCE) on the porous TiO₂ pellets prepared by sol–gel method in the single pass mode and demonstrated that undesirable byproducts were produced via Cl radical initiated mechanism.^{14,15} For these chloroethylenes, the catalytic activity of the TiO₂ pellets was maintained, whereas it decreased remarkably with an increase in the irradiation time for the

photocatalytic degradation of chloroform.¹⁶ To improve the usefulness of the TiO₂ photocatalyst, it is essential to understand the surface chemistry. In this study, we performed the photocatalytic degradation of chloroethanes to compare the data with those of chloroethylenes. We describe that the photocatalytic activity of the TiO₂ decreases drastically during the photodegradation of chloroethanes, and surface acidity on the catalyst affects the photocatalytic performance.

Experimental Methods

Ethane, chloroethane, or 1,2-dichloroethane (500 ppmv, balance nitrogen, Sumitomo Seika Chemicals Co.), nitrogen (99.999%), oxygen (99.999%), and synthesized air (oxygen 20.0 to 21.5%) were used as received from compressed gas cylinders. Humidified air was prepared by bubbling gas through a glass saturator containing deionized water. Water content was fixed as a result of controlling temperature and the flow rate of the gas stream passing through the saturator. Porous TiO₂ pellets were prepared by sol–gel techniques and fired at 200 °C.⁸ The specific surface area and porosity of these materials were 154 m² g⁻¹ and 50%, respectively, as obtained by the BET analysis.

The photodegradation experiments were carried out in a packed bed tubular photoreactor (Pyrex, 11.5 cm long, 0.24 cm i.d., and 0.32 cm o.d.) in a noncirculating mode. Four 4 W fluorescent black light bulbs (Toshiba, FL 4BLB) surrounded the tubular reactor. The photon flow rate (wavelength <400 nm) entering the reactor was determined to be 1.7×10^{-7} einstein s⁻¹ using a uranyl oxalate actinometer.⁸ All experiments except for examining an effect of temperature were conducted at room temperature, and air was passed around the reactor to avoid the temperature of the pellets from rising by illumination.

The concentrations of ethane, chloroethane, and 1,2-dichloroethane as reactants and CO₂, ethylene, and vinyl chloride as products in the gas stream were analyzed by gas chromatography (Hewlett-Packard 5890 series II equipped with a Porapak R

* Corresponding author. Tel/Fax: +81-83-933-5763. E-mail: yamazaki@yamaguchi-u.ac.jp.

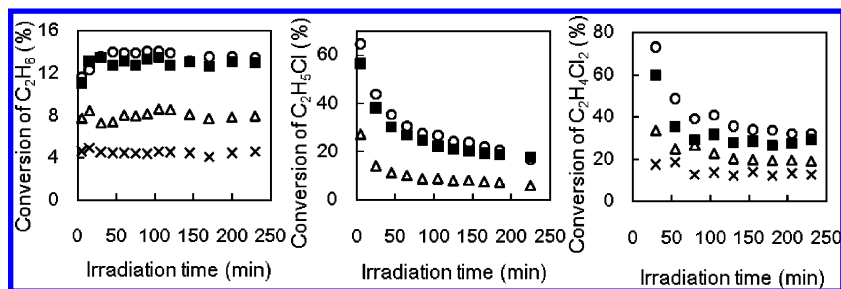


Figure 1. Time course of conversion of C_2H_6 , C_2H_5Cl , and $C_2H_4Cl_2$ on the TiO_2 of 0.1 (\times), 0.2 (Δ), 0.3 (\blacksquare), and 0.4 (\circ) g. The mole fraction of C_2H_6 , C_2H_5Cl , or $C_2H_4Cl_2$ was 1.64×10^{-4} , and that of oxygen and water vapor were 0.21 and 1.57×10^{-3} , respectively. The flow rate was 42 mL min^{-1} .

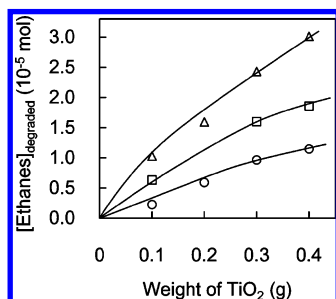


Figure 2. Comparison of the degraded amounts of C_2H_6 (\circ), C_2H_5Cl (\square), and $C_2H_4Cl_2$ (Δ). Other conditions were the same as those in Figure 1.

column using flame ionization and thermal conductivity detectors). Reactant or product gas stream was introduced to the gas chromatograph through six-port injection valves, one of which was connected to a sample loop of $250 \mu\text{L}$. Ion chromatography (Shimadzu, PIA-1000) was used to determine Cl^- ions, which were formed by immersing catalysts into water after the photodegradation experiments. The organic products adsorbed on the catalyst surface were extracted into methanol and were analyzed by GC/MS (HP 5890/HP 5970B) operating in the electron impact mode using a $60 \text{ m} \times 0.25 \text{ mm} \times 1.0 \mu\text{m}$ film thickness Aquatic column. Measurements of diffuse reflectance infrared Fourier transform (DRIFT) spectra were performed by utilizing a FTIR spectrophotometer (Nicolet AVATAR 370 DTGS) equipped with a DRIFT accessory (AVATAR Collector II).

Results and Discussion

In a continuous flow system with a noncirculating mode, reactant's concentrations decrease with an increase in an irradiation time and reach constant values. Conversion and stoichiometric ratio are determined after such a steady-state condition is established. Such a behavior was obtained for the photodegradation of ethane. However, in the photodegradation of C_2H_5Cl or $C_2H_4Cl_2$, the reactants' concentration in an effluent gas stream decreased instantly by irradiation but then increased gradually with an increase in the irradiation time. This fact indicates that conversion (defined as the reactant's molar flow rate degraded divided by the inlet reactant's molar flow rate) decreased with the irradiation time. Figure 1 shows dependences of the conversion on the irradiation time when 164 ppmv reactant gas stream containing 1.57×10^3 ppmv H_2O and 2.1×10^5 ppmv O_2 was passed through 0.10, 0.20, 0.30, or 0.40 g of the TiO_2 pellets at the flow rate of 42 mL min^{-1} . The total moles of the reactants degraded for the irradiation for 4 h were estimated by integrating the curves in Figure 1. Figure 2 indicates that the total moles of the reactant degraded on the TiO_2 increase with an increase in the amounts of TiO_2 , and the

TABLE 1: Stoichiometric Ratio and Products Adsorbed on the TiO_2 Surface

reactant	$[CO_2]_{\text{formed}}$	$[Cl^-]_{\text{formed}}$	products on TiO_2
	$[\text{ethanes}]_{\text{degraded}}$	$[\text{ethanes}]_{\text{degraded}}$	
C_2H_6	1.76 ± 0.04		HCOOH
C_2H_5Cl	1.63 ± 0.09	0.91	HCOOH, CH_3COOH , $CH_2ClCOOH$
$C_2H_4Cl_2$	1.13 ± 0.05	1.62	HCOOH, $CH_2ClCOOH$, $CHCl_2COOH$

reactant having more Cl atoms is degraded more easily, that is, $C_2H_4Cl_2 > C_2H_5Cl > C_2H_6$. Similar tendency was obtained for the degradation of chlorinated ethylenes, that is, $PCE > TCE > C_2H_3Cl > C_2H_4$.¹⁴ The stoichiometric ratio of $[CO_2]_{\text{formed}}/[C_2H_6]_{\text{degraded}}$, $[CO_2]_{\text{formed}}/[C_2H_5Cl]_{\text{degraded}}$, or $[CO_2]_{\text{formed}}/[C_2H_4Cl_2]_{\text{degraded}}$ was obtained to be 1.76 ± 0.04 , 1.63 ± 0.09 , or 1.13 ± 0.05 , respectively, indicating that 88.0% of C_2H_6 , 81.5% of C_2H_5Cl , and 56.5% of $C_2H_4Cl_2$ were mineralized. After passing the product gas stream successively through two water traps, each of which contained 100 mL of $0.023 \text{ mol dm}^{-3}$ aqueous NaOH solution, no appreciable Cl^- was detected in these traps. When the TiO_2 pellets were immersed into water after the photodegradation experiments for 4 h, the formation of Cl^- was confirmed by ion chromatography. The stoichiometric ratios of $[Cl^-]_{\text{formed}}/[C_2H_5Cl]_{\text{degraded}}$ and $[Cl^-]_{\text{formed}}/[C_2H_4Cl_2]_{\text{degraded}}$ were obtained to be 0.91 and 1.62, respectively, indicating that dechlorination percent of C_2H_5Cl and $C_2H_4Cl_2$ were 91.0 and 81.0%, respectively. It is also noted that HCOOH was detected as a very small peak in the ion chromatogram. These data on the stoichiometry suggest the formation of other organic products. The TiO_2 pellets after being used for the experiments were immersed in methanol, which was then analyzed by GC/MS. Chlorinated acetic acids were detected as products, as listed in Table 1.

Effect of Reaction Conditions. Effects of mole fractions of water vapor, O_2 , and the reactants and reaction temperature on the amounts of the degraded reactants were depicted in Figures 3–6. The presence of more water vapor gave less degradation of the reactants, suggesting that chlorinated ethanes and water vapor compete for adsorbing to the same sites on the TiO_2 . Figure 4 indicates that the degraded amount of the reactants in the absence of O_2 is relatively less than those in the presence of O_2 , but the mole fraction of O_2 does not affect the degraded amounts of the reactants significantly. However, the CO_2 formation was much less in the absence of O_2 , that is, $[CO_2]_{\text{formed}}/[C_2H_5Cl]_{\text{degraded}}$ or $[CO_2]_{\text{formed}}/[C_2H_4Cl_2]_{\text{degraded}}$ was 0.38 or 0.42, respectively. Figure 5 shows that more reactants are degraded as the mole fraction increases in the feed gas stream. Figure 6 indicates that more reactants are degraded at higher temperature. Qualitatively similar behaviors as Figures 3–5 were obtained for the degradation of chlorinated ethylenes.¹⁴ The effect of

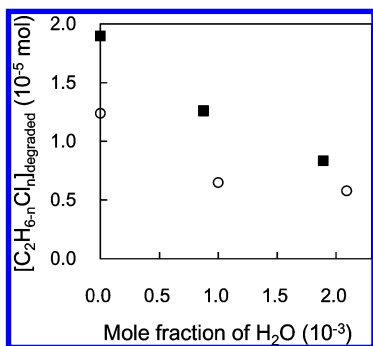


Figure 3. Effect of water vapor mole fraction on the amounts of the degraded C₂H₅Cl (○) and C₂H₄Cl₂ (■). Reaction conditions were the same as those in Figure 1 except for 0.1 g of TiO₂.

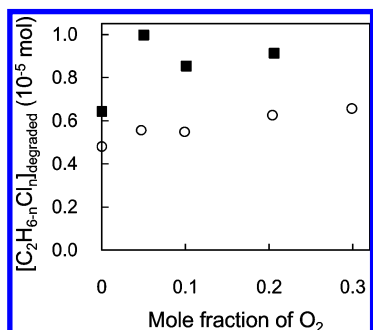


Figure 4. Effect of O₂ mole fraction on the amounts of the degraded C₂H₅Cl (○) and C₂H₄Cl₂ (■). Reaction conditions were the same as those in Figure 1 except for 0.1 g of TiO₂.

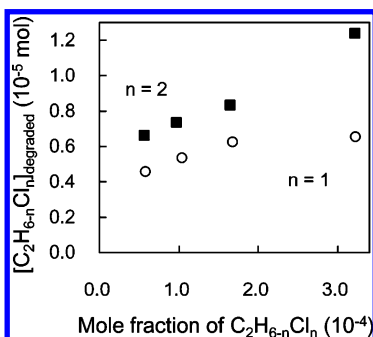


Figure 5. Effect of C₂H₅Cl or C₂H₄Cl₂ mole fraction on the amounts of the degraded C₂H₅Cl (○) and C₂H₄Cl₂ (■). Reaction conditions were the same as those in Figure 1 except for 0.1 g of TiO₂.

temperature was quite different for the degradation of chloroethylenes and chloroethanes. The degradation of chlorinated ethylenes was hardly affected by the temperature, whereas Figure 6 depicts that the degradation of C₂H₅Cl or C₂H₄Cl₂ at 84.3 °C is accelerated by a factor of 2.1 or 1.6 from that at 29.6 °C, respectively.

A reaction mechanism, as shown in Scheme 1, is proposed to account for the formation of the products listed in Table 1. In the photodegradation of organic compounds on the TiO₂ photocatalyst, the photogenerated holes react with adsorbed water molecules to form OH radicals, which abstract H radicals from chloroethanes. It is also likely that the photogenerated holes oxidize chloroethanes, followed by elimination of H⁺, leading to the formation of carbon-centered radicals CH₂CH₂Cl or CH₃CHCl from C₂H₅Cl and CH₂ClCHCl from C₂H₄Cl₂. The obtained carbon-centered radicals subsequently react with oxygen to form peroxy radicals. These species are converted to chloroethoxy radicals by reaction with a second peroxy radical. The elimination of H or Cl radicals from the chlorinated ethoxy radicals leads to the formation of CH₂CICOOH (pathway

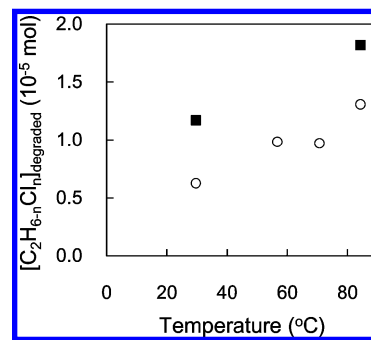
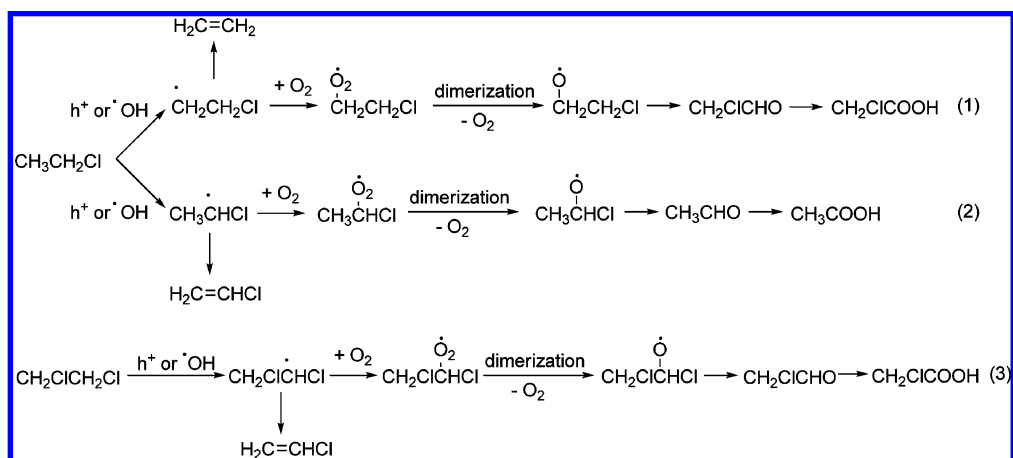


Figure 6. Effect of reaction temperature on the amounts of the degraded C₂H₅Cl (○) and C₂H₄Cl₂ (■). Reaction conditions were the same as those in Figure 1 except for 0.1 g of TiO₂.

(1) or CH₃COOH (pathway (2)) from C₂H₅Cl, and the elimination of Cl radicals yields CH₂CICOOH from C₂H₄Cl₂ (pathway (3)). There are two pathways for the degradation of C₂H₅Cl. After the photodegradation experiment was performed by passing the reactant gas stream containing 164 ppmv C₂H₅Cl, 2.04 × 10³ ppmv O₂, and 1.50 × 10³ ppmv H₂O through 0.1 g of TiO₂ pellets at the flow rate of 45 mL min⁻¹ for 155 min, 0.05 g of the TiO₂ pellets was immersed in 0.1 mL of methanol for 24 h. Then, the methanol was analyzed by GC-MS. Because 44.8 nmol of CH₃COOH and 0.240 nmol of CH₂CICOOH were detected, pathway (2) is predominant to pathway (1). When the same experiments were carried out for the degradation of C₂H₄Cl₂, 70.6 nmol of CH₂CICOOH and 0.238 nmol of CHCl₂COOH were detected. The formation of CHCl₂COOH cannot be explained in Scheme 1. Possibly, the carbon-centered radical, CH₂ClCHCl, might convert to vinyl chloride by dechlorination, followed by the addition of Cl radical to form CH₂CHCl₂ radical, which reacts with oxygen to form CHCl₂COOH via CHCl₂CHO. Formate is known as an intermediate produced during the photocatalytic oxidation of acetate to CO₂.¹⁷ When the photodegradation experiments were performed in the absence of O₂ in the feed gas stream, the formation of C₂H₄ and C₂H₃Cl from C₂H₅Cl and C₂H₃Cl from C₂H₄Cl₂ was detected. The formation of these alkenes can be explained in terms of the elimination of H or Cl radical from the carbon-centered radicals in Scheme 1. The concentrations of these alkenes were quite small because the photocatalytic activity of the TiO₂ drastically decreased in the absence of O₂, as shown in Figure 7. Figure 8 indicates that the amounts of the degraded C₂H₅Cl or C₂H₄Cl₂ are not affected by the reaction temperature, whereas the formation of these products is accelerated at higher temperature. It is worthy to note that ethylene and vinyl chloride are useful raw materials in chemical industries, although further study is needed to improve the conversion to these alkenes.

After the photodegradation of C₂H₅Cl for 4 h, all of the TiO₂ pellets were washed thoroughly with water to remove the adsorbed products and were dried in a desiccator with silica gels. Then, the pellets were packed into the photoreactor, and the experiment was conducted again. The time course of C₂H₅Cl conversion in the second run was almost the same as that in the first run, as shown in Figure 9. This finding indicates that an activity of the TiO₂ was recovered by washing with water, suggesting that a deactivation of the photocatalyst is due to the adsorption of the products on the surface. As mentioned above, the amount of Cl⁻ detected on the TiO₂ pellets was 91.0% of the degraded C₂H₅Cl, and 81.5% of the degraded C₂H₅Cl was mineralized to CO₂. The latter fact suggests that 18.5% of the degraded C₂H₅Cl was converted to organic products such as HCOOH, CH₃COOH, and CH₂CICOOH. Therefore, Cl⁻ is the

SCHEME 1



main product adsorbed on the TiO_2 surface. We prepared HCl-adsorbed TiO_2 pellets (Cl^-/TiO_2) by placing 0.56 g of the fresh TiO_2 pellets into 40 mL of 1.27 mol dm^{-3} aqueous HCl solution, followed by filtration and drying. The photodegradation of $\text{C}_2\text{H}_5\text{Cl}$ on the Cl^-/TiO_2 is depicted in Figure 9, where the conversion is maintained to be as low as $19.30 \pm 1.34\%$. This finding indicates that the adsorption of HCl causes the deterioration of the photocatalytic activity in the degradation of $\text{C}_2\text{H}_5\text{Cl}$.

Effect of Surface Acidity. Monitoring pyridine adsorption with FTIR is a widely used method of observing the presence of Lewis and Brønsted acid sites on catalysts.^{18–21} The commonly accepted procedure for FTIR spectral interpretation of pyridine adsorbed on TiO_2 and zeolites attributes absorption at $1540\text{--}1545 \text{ cm}^{-1}$ to pyridine adsorbed at Brønsted sites, whose adsorbed structure is pyridinium ion. Figure 10a shows DRIFT spectra of pyridine adsorbed on the fresh TiO_2 , and the peaks at 1605 , 1490 , and 1443 cm^{-1} were attributed to pyridine adsorbed on Lewis sites.^{22–24} On the TiO_2 after being used for the photodegradation of $\text{C}_2\text{H}_5\text{Cl}$, new peaks were detected at 1574 and 1545 cm^{-1} as shown in Figure 10b, suggesting the formation of Brønsted sites during the photodegradation. The peak at 1574 cm^{-1} was attributable to HCl adsorbed on the TiO_2 since it was observed when the fresh TiO_2 pellets were immersed in aqueous HCl solution, followed by filtration and dryness. Considering similarly to the model for strong Brønsted acidity induced by treatment of alumina with HCl,^{24,25} a possible structure of the Brønsted site can be proposed, as in Scheme 2.

Gaseous HCl can adsorb dissociatively to Ti–O sites or associatively to Ti sites. The Ti atom accepts the pair of electrons on a Cl^- ion. At the same time, the complementary proton bonds with the neighboring oxygen atom, leading to the formation of the Brønsted site. Molecularly adsorbed HCl also causes the Brønsted acidity.

Sulfated TiO_2 has been known as a solid acid catalyst and is being studied extensively in an effort to replace liquid-phase acids.^{19–23} It has been proposed that the strong acid property is related to sulfate ions and that high electron negativity of sulfur can induce polarization of neighboring OH groups, as shown in Scheme 3.^{19,20} As a result, the sulfated TiO_2 has Brønsted sites. We synthesized sulfated TiO_2 pellets ($\text{SO}_4^{2-}/\text{TiO}_2$) to examine whether the presence of Brønsted sites suppresses the photocatalytic degradation of $\text{C}_2\text{H}_5\text{Cl}$. The $\text{SO}_4^{2-}/\text{TiO}_2$ pellets were prepared by placing the fresh TiO_2 pellets into $0.050 \text{ mol dm}^{-3}$ sulfuric acid solution, followed by filtration and drying in a desiccator for 2 days.^{18,21} Figure 11a indicates the peak at 1546 cm^{-1} attributable to the Brønsted sites on the $\text{SO}_4^{2-}/\text{TiO}_2$ pellets. The peak at ca. 1600 cm^{-1} attributable to the Lewis sites is not observed because of a broad peak centered at 1640 cm^{-1} , pertaining to H–O–H bending for molecular water.²⁶ Figure 11b depicts the photodegradation of $\text{C}_2\text{H}_5\text{Cl}$ on the TiO_2 and $\text{SO}_4^{2-}/\text{TiO}_2$. It is noted that the conversion of $\text{C}_2\text{H}_5\text{Cl}$ maintained to be $14.40 \pm 0.17\%$ on the $\text{SO}_4^{2-}/\text{TiO}_2$, whereas it decreased from 39.4 to 12.9% on the TiO_2 during the irradiation for 4 h. This finding indicates that the $\text{C}_2\text{H}_5\text{Cl}$ adsorbed on the Lewis sites is degraded more effectively than that on the Brønsted sites, and the deterioration of the catalytic activity of the TiO_2 during the photodegradation of $\text{C}_2\text{H}_5\text{Cl}$ is due to the formation of the Brønsted sites on the surface.

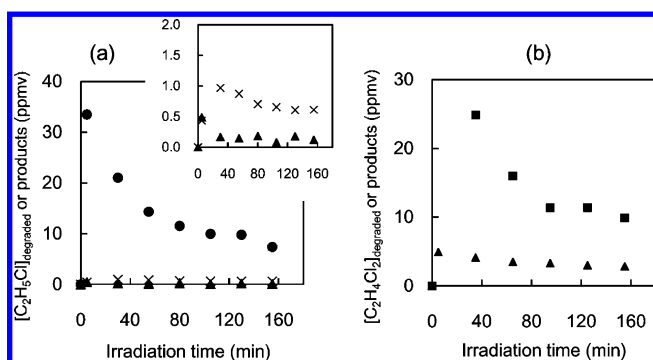


Figure 7. Time course of the reactants and products for the photocatalytic degradation of (a) $\text{C}_2\text{H}_5\text{Cl}$ or (b) $\text{C}_2\text{H}_4\text{Cl}_2$ in the absence of oxygen. The experiments were conducted on 0.1 g of TiO_2 at $70.7 \text{ }^\circ\text{C}$, and other conditions were the same as those in Figure 1. (a) $\text{C}_2\text{H}_5\text{Cl}$ (\bullet), $\text{C}_2\text{H}_3\text{Cl}$ (\blacktriangle), C_2H_4 (\times). The inset was magnification in the region of the low concentration below 2 ppmv . (b) $\text{C}_2\text{H}_4\text{Cl}_2$ (\blacksquare), $\text{C}_2\text{H}_3\text{Cl}$ (\blacktriangle).

For the photocatalytic degradation of chlorinated ethylenes such as vinyl chloride, TCE, or PCE, the conversion did not decrease but maintained during the irradiation. The formation of mono-, di-, and trichloroacetic acid was confirmed as a byproduct from vinyl chloride, TCE, or PCE, respectively.¹⁴ The accumulation of HCl on the TiO_2 pellets was also confirmed during the photocatalytic degradation of these chlorinated ethylenes.¹⁴ Figure 12a depicts the time course of the TCE conversion on the TiO_2 and the $\text{SO}_4^{2-}/\text{TiO}_2$ pellets, and both of them maintained to be almost constant. Figure 12b shows the DRIFT spectra of the TiO_2 pellets with and without the treatment with pyridine after the photodegradation of TCE. It should be noted that the spectrum without the treatment with pyridine showed two peaks at 1605 and 1411 cm^{-1} . These peaks can be assigned to asymmetric and symmetric stretching of

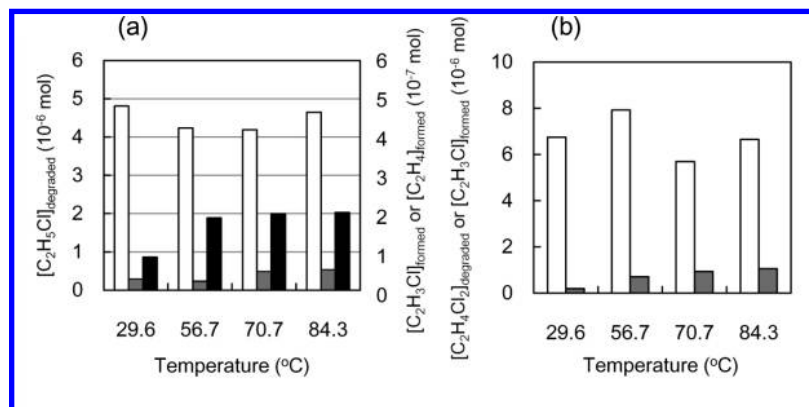


Figure 8. Effect of temperature on the amounts of the degraded reactants and of the products. (a) C_2H_5Cl (\square), C_2H_3Cl (shaded gray square), C_2H_4 (\blacksquare). (b) $C_2H_4Cl_2$ (\square), C_2H_3Cl (shaded gray square).

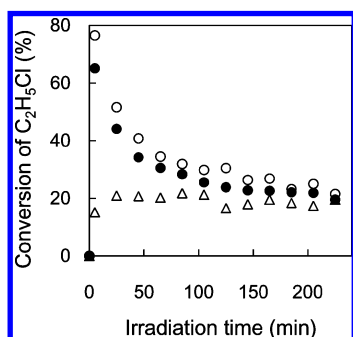


Figure 9. Photocatalytic degradation of C_2H_5Cl on fresh TiO_2 (\circ), the TiO_2 pellets washed with water after the photodegradation of C_2H_5Cl (\bullet), and the Cl^-/TiO_2 pellets (\triangle).

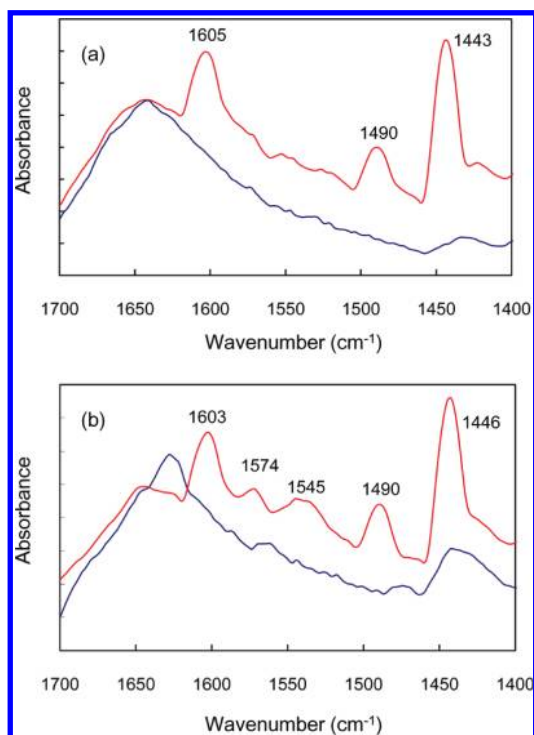
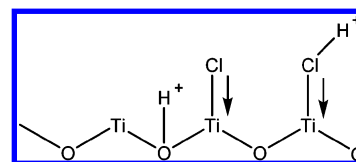


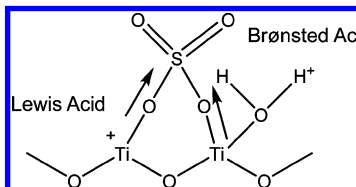
Figure 10. FTIR spectra of pyridine adsorbed on the TiO_2 pellets (a) before and (b) after the photodegradation of C_2H_5Cl . Unlabeled curves in parts a and b were FTIR spectra of the TiO_2 pellets without adsorbing pyridine.

COO^- , which comes from the reaction products, chloroacetates, accumulated on the TiO_2 surface.⁸ The DRIFT spectrum of pyridine adsorbed on the TiO_2 pellets indicates the peak at 1540 cm^{-1} , suggesting the formation of Brønsted sites. Therefore,

SCHEME 2



SCHEME 3



the photodegradation of TCE was not suppressed by the formation of Brønsted sites on the TiO_2 surface. This finding is also supported by the fact that a remarkable difference observed in the initial stage for the photodegradation of C_2H_5Cl , that is, 39.4% on the TiO_2 and 14.4% on the SO_4^{2-}/TiO_2 , was not observed for that of TCE. Figure 12a shows that the conversion is maintained to be 60.02 ± 0.78 or $46.37 \pm 0.32\%$ on the TiO_2 or the SO_4^{2-}/TiO_2 , respectively. Therefore, it is concluded that the existence of Brønsted sites hardly affects the degradation of TCE.

Conclusions

Photocatalytic degradation of gaseous chlorinated ethanes on the porous TiO_2 pellets was performed in a single pass mode. The steady-state condition was not obtained, but the deterioration in the photocatalytic activity was observed during the irradiation. On the basis of the products detected with and without oxygen

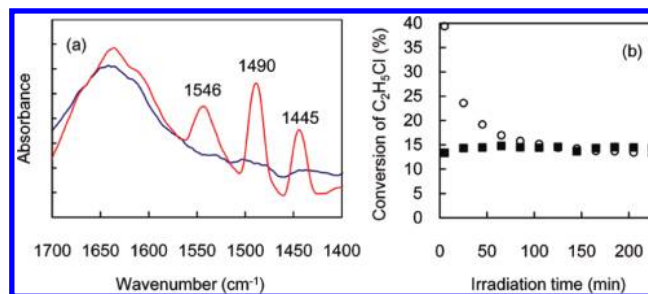


Figure 11. Photocatalytic degradation of C_2H_5Cl on the SO_4^{2-}/TiO_2 pellets. (a) FTIR spectra with and without the treatment with pyridine. (b) Time course of the conversion on the SO_4^{2-}/TiO_2 (\blacksquare) or the TiO_2 pellets (\circ).

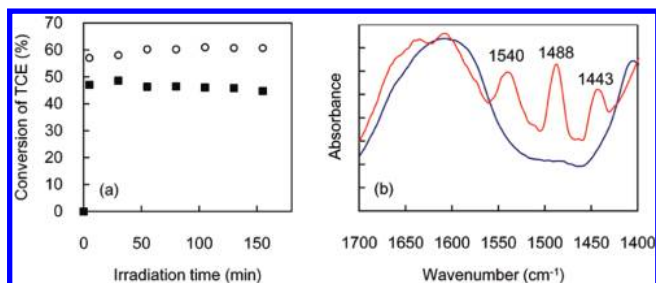


Figure 12. Photocatalytic degradation of TCE. (a) Time course of the conversion on the SO₄²⁻/TiO₂ (■) or the TiO₂ pellets (○). (b) FTIR spectra with and without the treatment with pyridine after the photodegradation of TCE was conducted on the TiO₂ pellets.

in the reactant's gas stream, we propose the degradation mechanism, as shown in Scheme 1. The decrease in the conversion for the photodegradation of C₂H₅Cl is attributable to the formation of Brønsted sites. Comparison of the data obtained with the TiO₂ and the SO₄²⁻/TiO₂ pellets indicates that the photodegradation of C₂H₅Cl is suppressed by the presence of the Brønsted sites, but that of TCE is not affected. Such a difference might be due to the adsorption process of these reactants on the TiO₂ surface. In heterogeneous TiO₂ photocatalysis, organic compounds tend to be oxidized adsorb on active surface sites competitively with water. The adsorption of water on TiO₂ has been well studied.^{27–29} It has been postulated that H₂O dissociates into OH⁻ ions that adsorb via their O end on top of five-fold coordinated surface Ti ions (Lewis sites), with the other H⁺ ion bonding to a lattice O ion to form a second type of adsorbed OH⁻ species.³⁰ Therefore, TCE and C₂H₅Cl adsorb on Lewis sites in the dark before irradiation. The correlation between the type of acidity (Brønsted or Lewis) and catalyst activity has been debated in conversion reactions of hydrocarbons derived from petroleum, that is, alkylation, isomerization, and cracking.²² Alkenes chemisorb on acidic solids like silica–alumina through the acceptance of a proton from Brønsted sites. Alkanes are not chemisorbed effectively on moderately acidic solids, and methane and ethane are not chemisorbed on silica–alumina.²⁴ In the photocatalytic degradation of chlorinated ethanes on the TiO₂ pellets, the Brønsted sites form because of the accumulation of acidic products, leading to the suppression of the adsorption of the chloroethanes. Therefore, as the reaction proceeds, the C₂H₅Cl conversion decreases because of the decrease in the chemisorbed species on Lewis sites and reaches a new steady-state on the formed Brønsted sites. Indeed, after 0.02 g of the TiO₂ pellets or those that had been used for the photodegradation of C₂H₅Cl were placed in a closed vessel containing 223 ppmv C₂H₅Cl for 1 h, the concentration of C₂H₅Cl in the gas phase was analyzed to examine the amount of the adsorbed C₂H₅Cl. As a result, (4.19 or 2.47) × 10⁻⁸ mol of C₂H₅Cl was adsorbed on the fresh or used TiO₂ pellets, respectively. On the contrary, the similar experiments using TCE instead of C₂H₅Cl indicated that the amount of adsorbed TCE on the used TiO₂ pellets did not decrease compared with those on the fresh ones. The effect of mole fractions of water vapor, O₂, and the reactants on the photodegradation of C₂H₅Cl and C₂H₄Cl₂ were qualitatively similar to those obtained for the photodegradation of chlorinated ethylenes. The reaction temperature significantly affected the degradation of chlorinated ethanes, although the degradation rates of TCE and PCE hardly depended on temperature.^{8,31} Such a temperature effect on chlorinated ethanes might be ascribed to adsorption of HCl or water, which is suppressed at higher temperature. Determination of the amount of the Brønsted sites

under various reaction temperatures is useful for understanding the effect of temperature. Lewis sites can be converted to Brønsted sites by interaction with a water molecule.²⁴ Therefore, water adsorbed on the TiO₂ surface must play an important role in accounting for the effect of temperature and the formation of Brønsted sites. We are continuing the research for discussing quantitatively the amount of chemisorbed species and the number of the Brønsted sites.

The acid–base property is one of the important surface chemical properties of the metal oxide catalysts. However, in the photocatalytic reaction of TiO₂, most of the studies have been discussed by using the Langmuir–Hinshelwood kinetics, where the number of the active sites initially present on the surface is fixed.³² Some investigators have reported that the deactivation observed in the photocatalytic oxidation of aromatic contaminants was ascribed to the accumulation of recalcitrant products on the catalyst surface.^{19,33} This article suggests that the modification of surface acid property by the interaction of the accumulated products is one of the reasons for the deactivation of the photocatalysts.

Acknowledgment. This work was partially supported by a Grant-in-Aid for Scientific Research (C) from the Ministry of Education, Culture, Sports, Science and Technology (MEXT) of the Japanese Government (20550179).

References and Notes

- Blake, D. M. *Bibliography of Work on the Heterogeneous Photocatalytic Removal of Hazardous Compounds from Water and Air*; Technical Report for National Renewable Energy Laboratory: Golden, CO, 2000.
- Phillips, L. A.; Raupp, G. B. *J. Mol. Catal.* **1992**, *77*, 297.
- Nimlos, M. R.; Jacoby, W. A.; Blake, D. M.; Milne, T. A. *Environ. Sci. Technol.* **1993**, *27*, 732.
- Yamazaki-Nishida, S.; Read, H. W.; Nagano, K. J.; Cervera-March, S.; Anderson, M. A. *J. Soil Contam.* **1994**, *3*, 363.
- Fan, J.; Yates, J. T., Jr. *J. Am. Chem. Soc.* **1996**, *118*, 4686.
- Hwang, S.-J.; Petucci, C.; Raftery, D. *J. Am. Chem. Soc.* **1998**, *120*, 4388.
- Kutsuna, S.; Ebihara, Y.; Nakamura, K.; Ibusuki, T. *Atmos. Environ.* **1993**, *27*, 599.
- Anderson, M. A.; Yamazaki-Nishida, S.; Cervera-March, S. In *Photocatalytic Purification and Treatment of Water and Air*; Ollis, D. F., Al-Ekabi, H., Eds.; Elsevier Science: Amsterdam, 1993; p 405.
- Yamazaki-Nishida, S.; Cervera-March, S.; Nagano, K. J.; Anderson, M. A.; Hori, K. *J. Phys. Chem.* **1995**, *99*, 15814.
- Yamazaki-Nishida, S.; Fu, X.; Anderson, M. A.; Hori, K. *J. Photochem. Photobiol., A* **1996**, *97*, 175.
- Hung, C.-H.; Marinas, B. *J. Environ. Sci. Technol.* **1997**, *31*, 562.
- Hung, C.-H.; Marinas, B. *J. Environ. Sci. Technol.* **1997**, *31*, 1440.
- Guo-Min, Z.; Zhen-Xing, C.; Min, X.; Xian-Qing, Q. *J. Photochem. Photobiol., A* **2003**, *161*, 51.
- Yamazaki, S.; Tanimura, T.; Yoshida, A.; Hori, K. *J. Phys. Chem.* **2004**, *108*, 5183.
- Tanimura, T.; Yoshida, A.; Yamazaki, S. *Appl. Catal., B* **2005**, *61*, 346.
- Yamazaki, S.; Yoshida, A.; Abe, H. *J. Photochem. Photobiol., A* **2005**, *169*, 191.
- Backes, M. J.; Lukaski, A. C.; Muggli, D. S. *Appl. Catal., B* **2005**, *61*, 21.
- Colon, G.; Sanchez-Espana, J. M.; Hidalgo, M. C.; Navio, J. A. *J. Photochem. Photobiol., A* **2006**, *179*, 20.
- Nakajima, A.; Obata, H.; Kameshima, Y.; Okada, K. *Catal. Commun.* **2005**, *6*, 716.
- Yang, R. T.; Li, W. B.; Chen, N. *Appl. Catal., A* **1998**, *169*, 215.
- Arata, K. *Appl. Catal., A* **1996**, *146*, 3.
- Kulkarni, A. P.; Muggli, D. S. *Appl. Catal., A* **2006**, *302*, 274.
- Gomez, R.; Lopez, T.; Oritz-Islas, E.; Navarrete, J.; Sanchez, E.; Tzompanzti, F.; Bokhimi, X. *J. Mol. Catal. A: Chem.* **2003**, *193*, 217.
- Campbell, I. M. *Catalysis at Surfaces*; Chapman and Hall: New York, 1988.
- Lindblad, M.; Pakkanen, T. A. *Surf. Sci.* **1993**, *286*, 333.
- Wang, R.; Hashimoto, K.; Fujishima, A.; Chikuni, M.; Kojima, E.; Kitamura, A.; Shimohigoshi, M.; Watanabe, T. *Adv. Mater.* **1998**, *10*, 135.
- Nakamura, R.; Ueda, K.; Sato, S. *Langmuir* **2001**, *17*, 2298.

(28) Nosaka, A. Y.; Kojima, E.; Fujiwara, T.; Yagi, H.; Akutsu, H.; Nosaka, Y. *J. Phys. Chem. B* **2003**, *107*, 12042.

(29) Murakami, Y.; Kenji, E.; Nosaka, A. Y.; Nosaka, Y. *J. Phys. Chem. B* **2006**, *110*, 16808.

(30) Henrich, V. E.; Cox, P. A. *The Surface Science of Metal Oxides*; Cambridge University Press: New York, 1994.

(31) Yamazaki, S.; Tsukamoto, H.; Araki, K.; Tanimura, T.; Tejedor-Tejedor, I.; Anderson, M. A. *Appl. Catal., B* **2001**, *33*, 109.

(32) Lewandowski, M.; Ollis, D. F. *Appl. Catal., B* **2003**, *43*, 309.

(33) Einaga, H.; Futamura, S.; Ibusuki, T. *Appl. Catal., B* **2002**, *38*, 215.

JP911842T